

## Supplementary Information for

### Substrate Co-Doping Modulates Electronic Metal-Support Interactions and Significantly Enhances Single-Atom Catalysis

J. L. Shi,<sup>a</sup> J. H. Wu,<sup>b</sup> X. J. Zhao,<sup>a</sup> X. L. Xue,<sup>a</sup> Y. F. Gao,<sup>c,d</sup> Z. X. Guo,<sup>e,a\*</sup> and S. F. Li<sup>\*a</sup>

<sup>a</sup>*International Laboratory for Quantum Functional Materials of Henan, School of Physics and Engineering, Zhengzhou University, Zhengzhou, Henan 450001, China*

<sup>b</sup>*Department of Physics, Henan Institute of Education, Zhengzhou, 450046, China*

<sup>c</sup>*Department of Materials Science and Engineering, University of Tennessee, Knoxville, Tennessee*

*37996, USA*

<sup>d</sup>*Materials Science and Technology Division, Oak Ridge National Laboratory, Oak Ridge, Tennessee*

*37831, USA*

<sup>e</sup>*Department of Chemistry, University College London, London WC1H 0AJ, UK*

#### **This file includes:**

**S1: Details on the simulation methods**

**S2: The optimized geometric structures of Pd@TiO<sub>2</sub>(110) and the minimum energy path for CO oxidation on it.**

**S3: Average bond lengths of the Pd atom with the surface Ti and O atoms of the co-doped substrates before and after O<sub>2</sub> adsorption.**

**S4: Orbital analysis for the initial stages of O<sub>2</sub> adsorption on pure and co-doped Pd@TiO<sub>2</sub>(110)**

**S5: The reason why V-N co-doping slightly departs from the linear trend.**

## S1: Details on the simulation methods

The electronic wave functions were expanded in a plane wave basis with an energy cutoff of 500 eV. To obtain the correct band gap of the  $\text{TiO}_2$ , we used the DFT+U method with  $U=5.5$  eV (Note: our tests show that the choice of  $U$  values around 5.0 eV lead to negligible differences for the calculated results, such as the adsorption energy  $\text{O}_2$  molecule and reaction barrier for CO oxidation). The calculated lattice parameters for primitive rutile  $\text{TiO}_2$  unit cell are  $a = b = 4.662$  Å and  $c = 2.959$  Å, respectively, in good agreement with experimental result.<sup>1</sup> The rutile  $\text{TiO}_2(110)$  surface was simulated by a periodic four-layer  $c(4\times 2)$  slab model consisting of 192 atoms with  $\sim 13$  Å of vacuum in between the slabs. The k-space integration was carried out using a Monkhorst-Pack grid of  $2\times 3\times 1$   $k$  points in the surface Brillouin zone of the  $c(4\times 2)$  unit cell. All atoms except those in the bottom layer were allowed to relax along the calculated forces until all the residual force components were less than 0.01 eV/Å. In consideration of the experimental condition and previous calculations, we performed calculations that the Pd ad-atom is located in the vicinity of surface oxygen vacancy ( $V_{\text{O}}$ ) site of the rutile rutile  $\text{TiO}_2(110)$  which is denoted as  $\text{Pd@TiO}_2(110)$  throughout the document. For the interaction of the  $\text{O}_2$  ( $\text{CO}$ ) molecule with the  $\text{Pd@TiO}_2(110)$  catalyst, we initially placed the  $\text{O}_2$  ( $\text{CO}$ ) molecule about 4.5 Å away from the Pd atom followed by fully structural optimization. Bader charge analysis<sup>2</sup> is applied to evaluate the charge transfer.

## S2: The optimized geometric structures of $\text{Pd@TiO}_2(110)$ and the minimum energy path for CO oxidation on it.

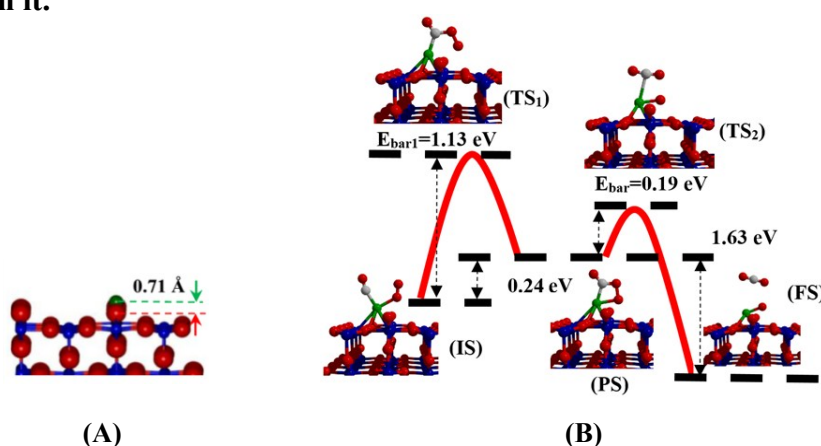


**Fig. S1** (color online) (A) The optimized geometric structures of  $\text{Pd@TiO}_2(110)$ ; (B) the minimum energy path for CO oxidation on  $\text{Pd@TiO}_2(110)$ . Note that though the Pd atom

prefers to locate in the oxygen vacancy site as presented in (A), upon O<sub>2</sub> and CO adsorption, the deposited Pd atom migrates slightly from the vacancy site, as shown in (B).

**S3: Average bond lengths of the Pd atom with the surface Ti and O atoms of the co-doped substrates before and after O<sub>2</sub> adsorption.**

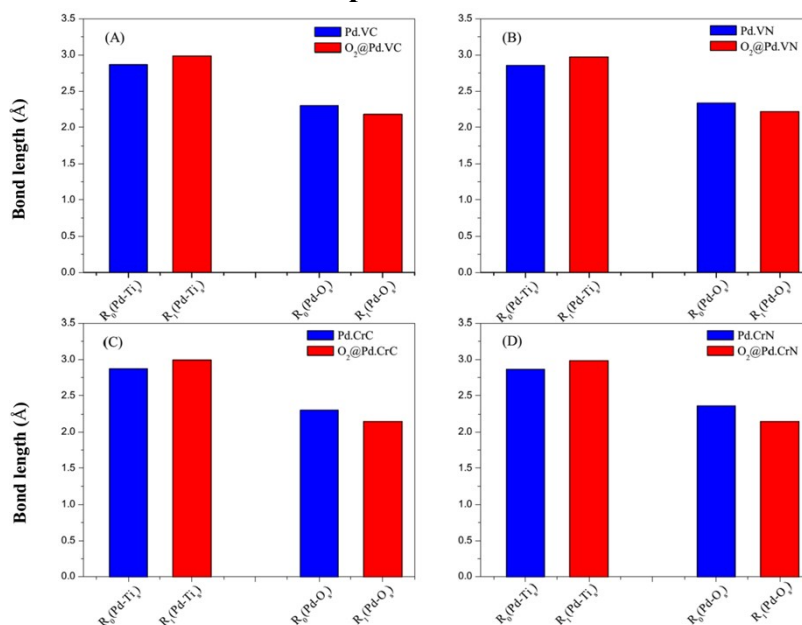


**Fig. S2.** Bond lengths of Pd atom with the Pd@TiO<sub>2</sub>(110) and O<sub>2</sub>-Pd@TiO<sub>2</sub>(110) complexes with (A) V-C; (B) V-N; (C) Cr-C; and (D) Cr-N co-dopant pairs.

In Fig. S2, we provide average bond lengths of the Pd atom with the surface Ti and O atoms of the co-doped substrates,  $R_i(\text{Pd-Ti}_s)$  and  $R_i(\text{Pd-O}_s)$ ;  $i=0$  and  $1$  correspond to the cases before and after O<sub>2</sub> adsorption on the supported Pd atom, respectively. One can readily see that the values of  $R_i(\text{Pd-Ti}_s)$  are increased after O<sub>2</sub> adsorption, however, the values for  $R_i(\text{Pd-O}_s)$  are decreased, indicating an weakened Pd-Ti<sub>s</sub> interaction and enhanced Pd-O<sub>s</sub> binding. To clearly illustrate the bond length changes, we summarize the calculated  $R_i(\text{Pd-Ti}_s)$  and  $R_i(\text{Pd-O}_s)$  in the table as follows:

Co-doped systems	$R_i(\text{Pd-Ti}_s)$ (Å)	$R_i(\text{Pd-O}_s)$ (Å)
Pd@TiO <sub>2</sub> :V-C	2.869	2.299
O <sub>2</sub> -Pd@TiO <sub>2</sub> :V-C	2.989	2.182
Pd@TiO <sub>2</sub> :V-N	2.858	2.337
O <sub>2</sub> -Pd@TiO <sub>2</sub> :V-N	2.975	2.218
Pd@TiO <sub>2</sub> :Cr-C	2.872	2.302
O <sub>2</sub> -Pd@TiO <sub>2</sub> :Cr-C	2.990	2.147
Pd@TiO <sub>2</sub> :Cr-N	2.863	2.356
O <sub>2</sub> -Pd@TiO <sub>2</sub> :Cr-N	2.982	2.148

#### S4: Orbital analysis for the initial stages of O<sub>2</sub> adsorption on pure and co-doped Pd@TiO<sub>2</sub>(110)

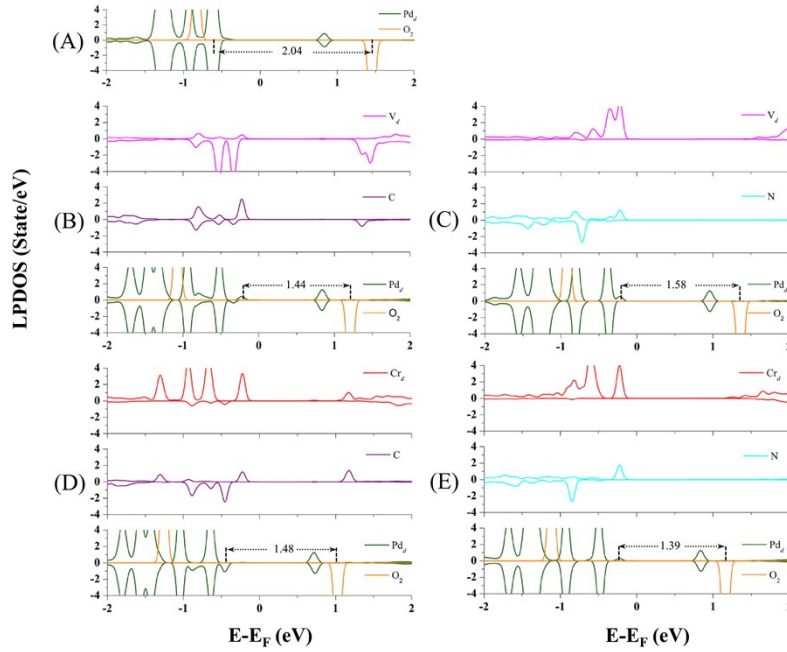


**Fig. S3.** (color online): Density of states (DOS) for the initial stages of an O<sub>2</sub> molecule approaching toward (A) Pd@TiO<sub>2</sub>(110), and co-doped with (B) V-C, (C) V-N, (D) Cr-C, and (E) Cr-N co-dopant pairs.

To clearly illustrate the effect of EMSI in improving the chemical activity of the Pd atom via co-doping, we analyze the DOS of the O<sub>2</sub> adsorption on Pd@TiO<sub>2</sub>(110) SAC and those co-doped with V-C, V-N, Cr-C, and Cr-N co-dopant pairs when the molecule is far (about 5.0 Å) above the Pd SACs, which can be viewed as the initial stages of the O<sub>2</sub> adsorptions in the present simulations. In general, we can see that the smaller the  $E_{\text{gap}}(\text{HOMO}(\text{Pd})\text{-LUMO}(\text{O}_2))$ , the larger the  $E_{\text{ads}}(\text{O}_2)$ , in close agreement with the well-known *d*-band theory<sup>3, 4</sup>. Note again that, the reduced  $E_{\text{gap}}(\text{HOMO}(\text{Pd})\text{-LUMO}(\text{O}_2))$  is originated from an enhanced EMSI through *n-p* co-doping: the stronger the EMSI, the smaller the  $E_{\text{gap}}(\text{HOMO}(\text{Pd})\text{-LUMO}(\text{O}_2))$ ; and consequently the stronger the O<sub>2</sub> activation.

Note that, we have also considered another type of *n*-type co-dopant pair, Cr-S, i.e., one Ti atom is replaced by a Cr atom, and one O is replaced by an S atom. In this situation, we found that Cr-S *n*-type co-doping (see **Fig. S4(A)** for the optimized structure) satisfied with the condition that the HOMO(Pd)-LUMO(O<sub>2</sub>) gap is located between the cases of V-N co-doping and Pd@Pristine TiO<sub>2</sub>(110). More specifically, in the cases of V-N co-doped and Pd@Pristine-TiO<sub>2</sub>(110), the

HOMO(Pd) -LUMO(O<sub>2</sub>) gaps are 1.58 and 2.04 eV, respectively, and in the Cr-S co-doped case the HOMO(Pd) -LUMO(O<sub>2</sub>) gap is 1.62 eV, as seen from the DOS presented from the **Fig.S4(B)** therein the O<sub>2</sub> is about 5 Å away from the Pd atom. Then, we further examine the O<sub>2</sub> adsorption and CO oxidation on the Cr-S co-doped Pd@TiO<sub>2</sub>(110), which is simply denoted as Pd@Cr-S@TiO<sub>2</sub>(110). In **Fig. S5**, we present the optimized geometric structure for O<sub>2</sub> adsorption on Cr-S co-doped Pd@TiO<sub>2</sub>(110), which is simply denoted as O<sub>2</sub>-Pd@Cr-S@TiO<sub>2</sub>(110). The calculated adsorption energy of the O<sub>2</sub> molecule (E<sub>ads</sub>(O<sub>2</sub>)) on Pd@Cr-S@TiO<sub>2</sub>(110) is 0.57 eV, which is well positioned on the linear relationship of the E<sub>ads</sub>(O<sub>2</sub>) as a function of the HOMO(Pd)-LUMO(O<sub>2</sub>) gap, as shown in the **Fig. 5** of the main text.

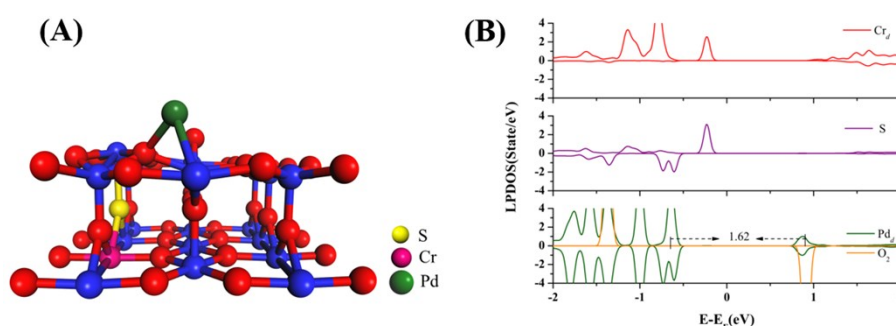


**Fig. S4:** (A) Optimized geometric structure of Cr-S co-doped Pd@TiO<sub>2</sub>(110), which is simply denoted as Pd@Cr-S@TiO<sub>2</sub>(110); (B) Local projected density of state (DOS) of the case when an incoming O<sub>2</sub> molecule is about 5 Å high above the deposited Pd atom.

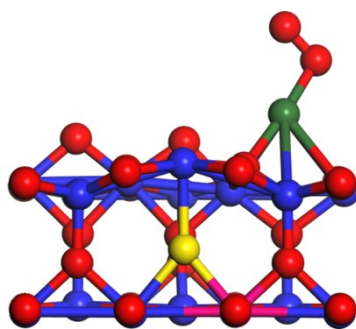


**Fig. S5:** Optimized geometric structure for O<sub>2</sub> adsorption on Cr-S co-doped Pd@TiO<sub>2</sub>(110).

### S5: The reason why V-N co-doping slightly departs from the linear trend.

After detailed analysis, we found that (in the **Fig. R3** or **Fig. 5**) the reduced reaction barrier for CO oxidation (E<sub>bar</sub>(CO oxidation)) in V-N co-doping relative to its neighboring cases, such as Cr-C and Cr-S co-doping, can be mainly due to the contrast energy changes upon the local geometric structure relaxations around the Pd single atom during the CO oxidation process.

More specifically, in the following **Fig. S6**, we present the local geometric structures of the initial states (IS) and transition states (TS) of the CO oxidation on Cr-C, V-N, and Cr-S co-doped Pd@TiO<sub>2</sub>(110) complexes in the left panels; correspondingly, for both the IS and TS structures, we have also performed static calculations on the energetics of the complexes in which the adsorbed CO and O<sub>2</sub> species are removed, as shown in the right panels. By doing this, we can estimate the geometric effect of the contrast relaxations around the Pd active site on the CO oxidation barriers of the studied systems. One can see that for both the cases of Cr-C and Cr-S co-doping, from the IS to the TS, the energy changes due to the local structural relaxations around the Pd atom are minor, approximately, 0.076 and 0.147 eV; however, for the case of V-N co-doping, the energy change is significant, by about 0.527 eV! Therefore, one can see that it is just such a contrast local geometric relaxation around the Pd single atom during the CO oxidation in the individual case of V-N co-doping as compared to other cases that results in the calculated  $E_{\text{bar}}(\text{CO oxidation})$  in **Fig. 5** departing from the exactly linear trend.

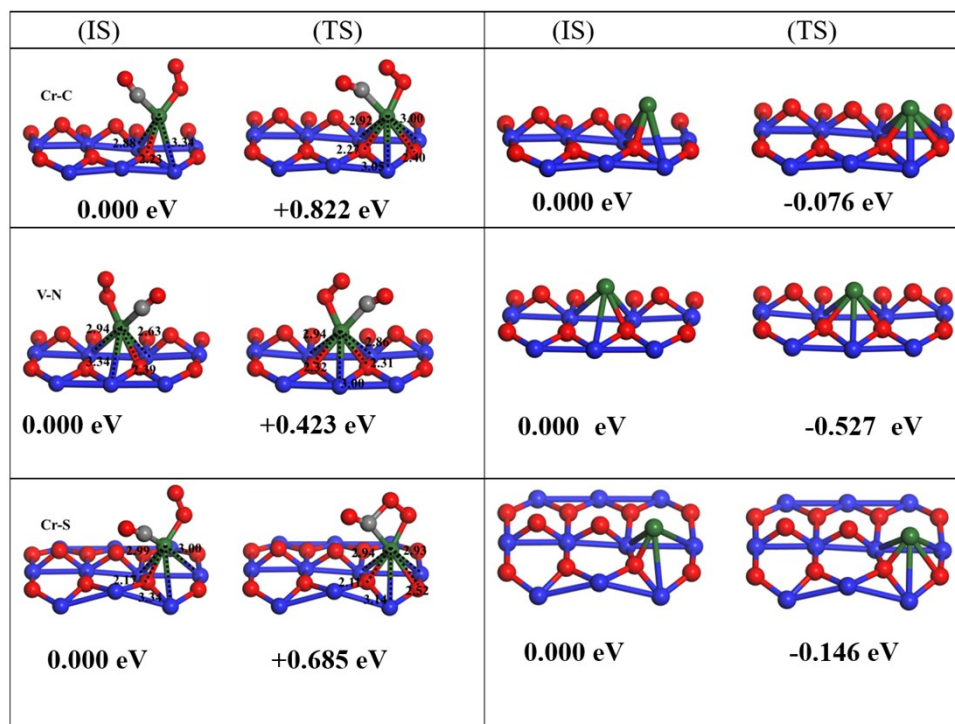


**Fig. S6:** Local geometric structures of the initial states (IS) and transition states (TS) for CO oxidation on Cr-C, V-N, and Cr-S co-doped Pd@TiO<sub>2</sub>(110) complexes, as shown in the left panels; Correspondingly, in the right panels, for both the IS and TS structures, we have also performed static calculations on the energetics of the complexes in which the adsorbed CO and O<sub>2</sub> species are removed meanwhile kept other atoms possessing the same structures as shown in the left panels.

1. J. K. Burdett, T. Hughbanks, G. J. Miller, J. W. Richardson and J. V. Smith, *J. Am. Chem.Soc.*, 1987, **109**, 3639-3646.
2. W. Tang, E. Sanville and G. Henkelman, *J. Phys.: Condens. Matter*, 2009, **21**, 084204.
3. B. Hammer, Y. Morikawa and J. K. Nørskov, *Phys. Rev. Lett.*, 1996, **76**, 2141-2144.
4. L. P. A. Nilsson, and J. K. Nørskov., *Chemical Bonding at Surfaces and Interfaces*, (Elsevier, Amsterdam, 2008).